Naked-eye detection of Staphylococcus aureus in powdered milk and infant formula using gold nanoparticles

Marco Marin, Francesco Rizzotto, Vincent Léguillier, Christine Péchoux, Elise Borezee-Durant, Jasmina Vidic

Naked-eye detection of *Staphylococcus aureus* in powdered milk and infant formula using gold nanoparticles

Marco Marin[1], Francesco Rizzotto[1], Vincent Léguillier[1], Christine Péchoux[2], Elise Borezee-Durant[1], Jasmina Vidic[1,*]

[1]Université Paris-Saclay, INRAE, AgroParisTech, Micalis Institute, 78350 Jouy-en-Josas, France.

[2]Université Paris-Saclay, INRAE, GABI, 78350 Jouy-en-Josas, France.

Corresponding author: (J.V.) Phone: +33134652737. E-mail: jasmina.vidic@inrae.fr

ABSTRACT

Nonspecific binding of proteins from complex food matrices is a significant challenge associated with a biosensor using gold nanoparticles (AuNPs). To overcome this, we developed an efficient EDTA chelating treatment to denature milk proteins and prevent their adsorption on AuNPs. The use of EDTA to solubilize proteins enabled a sensitive label-free apta-sensor platform for colorimetric detection of *Staphylococcus aureus* in milk and infant formula. In the assay, *S. aureus* depleted aptamers from the test solution, and the reduction of aptamers enabled aggregation of AuNPs upon salt addition, a process characterized by a color change from red to purple. Under optimized conditions, *S. aureus* could be visually detected within 30 min with the detection limit of 7.5×10^4 CFU/mL and 8.4×10^4 CFU/mL in milk and infant formula, respectively. The EDTA treatment provides new opportunities for monitoring milk contamination and may prove valuable for biosensor point-of-need applications.

Key words: gold nanoparticles, food matrix effect, aptamer, colorimetric detection.

1. INTRODUCTION

Staphylococcus aureus, commonly called “golden staph”, is a highly versatile human and animal pathogen and a major health concern due to accrued resistance to antibiotics. It is a Gram-positive opportunistic bacterium present on human skin and mucous in approximately 30% of the healthy population (Ryu et al. 2014). It is also frequently present in the air, dust, water and on environmental surfaces (Hennekinne et al. 2012). In humans and animals, *S. aureus* can cause different kinds of illnesses from minor skin infections to persistent intracellular infections and life-threatening septicemia. Additionally, it is the major cause of mastitis (Holmes and Zadoks 2011; Kadariya et al. 2014) which leads to the hygienic standards inadequacy for the human consumption of milk derived from animals affected by this illness. Finally, *S. aureus* has high potential for milk poisoning since it can produce seven different toxins that are heat resistant and survive pasteurization (Rajkovic et al. 2020).

Milk and dairy products are considered vehicles of *S. aureus* for infection in humans. The contamination may arrive along the production chain, during storage and distribution when hygienic milking conditions are not fully respected, but also via contaminated milking equipment (Hennekinne et al. 2012; Rubab et al. 2018). Cross-contamination by *S. aureus* during handling have been reported for powdered infant formula as well (Cho et al. 2019), which poses a serious health risk to newborns that do not have fully developed immune system. Efficient detection of *S. aureus* is of pronounce importance to prevent bacterium spread, and reduce risks associated with public health and food safety.

The traditional methods used for *S. aureus* detection are culture-based. They include sample preparation, enrichment, colony selection and enumeration, and a confirmation test (Cossettini et al. 2022; Vidic et al. 2019; Vizzini et al. 2019). Although accurate and sensitive, traditional methods are very laborious and need several days to yield results (Kotsiri et al.

2022; Ramarao et al. 2020; Vidic et al. 2017). Molecular technologies, such as MALDI-TOF mass spectroscopy, polymerase chain reaction (PCR), next generation sequencing, or enzyme-linked immunosorbent assay (ELISA), have also been developed (Kotsiri et al. 2022; Rubab et al. 2018). Although providing the result in several hours, molecular methods are not widely used because they require skilled staff and expensive laboratory facilities, and still frequently well-isolated colonies (Nouri et al. 2018; Vidic et al. 2019). Moreover, molecular methods may provide false negative results due to inhibitory activity of milk components on DNA polymerase and milk fat interferences in DNA extraction (Cossettini et al. 2022; Schrader et al. 2012; Vidic et al. 2020).

Over the last decade, nanotechnology has been increasing in relevance as an innovative tool for food safety assessment (Bobrinetskiy et al. 2021; Chen et al. 2018; Kumar et al. 2014). Different nanomaterial based assays have been develop to detect *S. aureus* including electrochemical (Eissa and Zourob 2020; Vidic and Manzano 2021; Xu et al. 2018), magnetic (Duarte et al. 2017; Martins et al. 2019), piezoelectric (Lian et al. 2015), and plasmonic (Abbaspour et al. 2015; Aura et al. 2017; Balbinot et al. 2021; Rüppel et al. 2018). Among plasmonic biosensors, those using gold nanoparticles (AuNPs) are particularly promising, because they can meet the international guidelines for diagnostics known as REASSURED (Real-time connectivity; Ease of specimen collection; Affordability; Sensitivity; Specificity; User-friendliness; Rapid & robust operation; Equipment-free; and Deliverability) (Land et al. 2019). AuNPs can be easily functionalized with biological molecules that ensure recognition (antibody, DNA), and allow a naked-eye detection of intact bacterial cells due to the Localized Surface Plasmon Resonance (LSPR) phenomenon (Marin et al. 2021). LSPR depends on the AuNPs refractive index that reflects nanoparticles size, morphology and inter-particle distance, as review recently (Marin et al. 2021). These parameters may be altered upon

AuNPs aggregation or upon particles binding to bacterial cells, which induce a color change of the particle solution: the more the distance between AuNPs is reduced upon aggregation, the intensity of the change in color from red to purple is greater.

However, although colorimetric LSPR biosensors enable rapid and point-of-need pathogen detection they can hardly be directly applied in complex food because of the inhibitory matrix effect (Chen et al. 2018). It was shown that matrix proteins could cause the loss of detection signals up to 80% in apta-sensors, immuno-sensors and fluorescent biosensors based on AuNPs (Tao et al. 2020).

The aim of this study was to develop and optimize an aptamer-based LSPR assay for *S. aureus* detection in milk and infant formula by improving both technology and sample treatment. Aptamers are short single-stranded oligonucleotides (DNA or RNA) that both recognize and bind to specific targets similarly as antibodies and adsorb on AuNPs (Zhang and Liu 2021). Milk products are among the most challenging food matrices for colorimetric tests because they contain components such as butterfat globules, carbohydrates, proteins, and various minerals (Quigley et al. 2013), that interact strongly with AuNPs and interfere with the assay result (Marin et al. 2021). By performing a single additional step prior to analysis to eliminate the matrix hindrance issue, a good LSPR sensor performance was demonstrated in both products. Our work demonstrates that the simple treatment opens the possibility for the rapid and naked-eye detection of *S. aureus* in milk products at the point-of-need.

2. MATHERIALS AND METHODS

2.1. Chemicals and reagents. AuNPs (10 nm), ethylenediaminetetraacetic acid (EDTA), Triton X100, hydrochloric acid (HCl), trichloroacetic acid (TCA) and phosphate buffered saline (PBS) were purchased from Sigma-Aldrich (Saint Quentin Fallavier, France) in analytical grade. AuNPs (20 nm), were purchased from Thermo Fisher Scientific (Illkirch, France). Powdered milk (Laboratoires Novalac SA, Genève, Switzerland) and infant formula (Novalec1) were purchased in the local supermarket. Aptamers were obtained from Eurofins Genomics SAS (Nantes, France). The specific anti-*S. aureus* aptamer (Apt1) was previously selected(Abbaspour et al. 2015) and had the following sequence: 5'-TCC CTA CGG CGC TAA CCC CCC CAG TCC GTC CTC CCA GCC TCA CAC CGC CAC CGT GCT ACA AC-3', while the control linear DNA (Campy) was 5'- GGG AGA GGC AGA TGG AAT TGG TGG TGT AGG GGT AAA ATC CGT AGA -3'. The stock solutions of the aptamers (100 µM) were prepared using miliQ water and kept at −20 °C until use.

2.2. Bacterial strains. All strains used in this study are listed in Table 1. Strains were grown in brain-heart-infusion (BHI) medium, Becton Dickinson (DB, Le Pont de Claix, France), with shaking at 37°C or on BHI agar at 37°C.

Table 1. Bacterial strains used in this study.

Microorganisms	Collection code
Staphylococcus aureus	FPR3757 USA300 [A]
Escherichia coli K12	ATCC 14948 [B]
Salmonella enteritidis	405/2006 [C]
Bacillus cereus	ATCC 14579 [B]
B. cereus S51	S51 [C]
Pseudomonas aeruginosa	ATCC 27853 [B]
Klebsiella pneumoniae	ATCC 700603 [B]
Bacillus cytotoxicus	NVH 391-98 [D]

Source/Reference: [A],(Schlag et al. 2007); [B], American Type Culture Collection (Manassas, VA, USA) [C], INRAE collection (Jouy en Josas, France); [D], (Lund et al. 2000).

2.3. Milk treatments. Powdered milk or infant formula was solubilized with milliQ water to obtain 1% solution and inoculated with bacterial cells. Bacterial cells were collected carefully from an overnight culture by centrifugation at 3000 rpm for 5 min, at room temperature and washed twice in PBS. Inoculates (500 µL), containing different bacterial concentrations, were added to 25 mL of milk or infant formula samples in a 250 mL Erlenmeyer flask. Flasks were incubated with shaking (200 rpm) at 37 °C for at least 30 min before testing.

After incubation, 3 ml of each sample were treated with (i) a double volume of 15 mM EDTA (pH 8 or 12) to denature proteins, (ii) 1M HCl until reaching pH 3 to solubilize proteins; (iii) 600 µL of 10% TCA to precipitate proteins; or (iv) a double volume of 15 mM EDTA, pH 8 with 1% Triton X100 to solubilize proteins and fats. Samples were incubated for 10 min, then centrifuged at 10,000 rpm x 15 minutes and pellets were resuspended in 1 mL PBS before being analyzed by the aptasensor.

To estimate bacterial survival, the drop plate method was performed in order to compare bacterial concentration in treated and untreated in milk/infant formula samples. The final numbers of bacteria were determined using a drop plate method. For this, the inoculated solution was serially diluted by placing 100 µL of the suspension into a dilution tube containing 900 µL of PBS. This tube was vortexed, and 100 µL was removed and placed into a second dilution tube containing 900 µL of PBS. This process was repeated six times. Then, 10µL of each dilution was plated on BHI agar and incubated for 18 h at 37 °C under aerobic condition. Colony counts from triplicate plates were converted to colony forming units/mL (CFU/mL).

144 **2.4. Imaging bacterial cells**. Bacteria viability in treated milk samples was estimated
145 using a LIVE/DEAD BacLight kit (ThermoFisher, Ilkrich, France) and an AxioObserver.Z1 Zeiss
146 optical microscope equipped with a Zeiss AxioCam MRm digital camera. The ZEN software
147 package was used to process the images.

148 TEM analysis were performed to visualize interaction of *S. aureus* cells with AuNPs using
149 a Hitachi HT7700 electron microscope operated at 80 kV (Elexience, France). Five µL of
150 bacterial solution (10^6 CFU/mL) were added to 50 µL of AuNPs, and 5 µL PBS and incubated
151 for 10 min. Then, 5 µL of 2M $MgCl_2$ were added to aggregate nanoparticles. Two µl of the
152 solution were collected onto 200-mesh copper grids, and visualized. Digital images were
153 acquired using a charge-coupled device camera system (AMT).

154 **2.5. Spectrophotometry.** The specificity of Apt1 binding to *S. aureus* cells was evaluated
155 using an UV-Vis spectrophotometer Biochrom Libra S22 (Biochrom Ltd., Cambridge, UK).
156 Bacterial cells were washed and resuspended in 0.1 mM EDTA, 10 mM Tris-HCl, pH 8, to final
157 concentration of 10^6 CFU/mL. *S. aureus* cells were incubated with 5 µM of Atp1 at 37°C for 1
158 h in stirring conditions. Subsequently, bacterial cells were centrifuged at 3000 rpm x 5 min,
159 the supernatant was removed and the pellet was resuspended in PBS for analysis. In control
160 experiments, Apt1 was replaced by the linear DNA oligomer.

161 **2.6. Aptasensor optimization.** Optimization of the aptamer concentration was carried
162 out using 50 µL of AuNPs solution (20 nm), 5 µL of PBS and 5 µL of different aptamer
163 concentrations (ranging from 0 to 16.9 µM). After 10 min incubation under gentile shaking, 5
164 µL of 2 M $MgCl_2$ were added and the color change of the solutions was evaluated by
165 measuring absorption at 520 nm and 630 nm (A630/A520) using Tecan plate reader (Tecan
166 Infinite M200PRO, Männedorf, Switzerland).

2.7. Detection of *S. aureus*. Milk and infant formula were spiked with different concentrations of *S. aureus* (0 to 10^8 CFU/mL). Subsequently, 3 mL of each sample was treated with 6 mL of 15 mM EDTA, pH 8, centrifuged and resuspended in 1 mL PBS. Fifteen µL of resuspended bacterial cells was incubated with Apt1 (2 µM) for 10 min, then centrifuged at 3000 × rpm for 5 min. The supernatant containing unbound aptamer (5 µL) was incubated with 50 µL of AuNPs (0.27 pM). After equilibrating solutions at room temperature for 10 min, 5 µL of 2 M $MgCl_2$ were added, mixed, and incubated for another 15 min. Then, the solution was transferred to a 96-well plate for spectral recording using plate reader. All assays were performed at room temperature.

3. RESULTS AND DISCUSSION

3.1. Binding of Apt1 to *S. aureus*. Recognition of *S. aureus* cells by Apt1 was tested by UV-Vis spectroscopy. Apt1, as a DNA, has a maximum absorption at 260 nm (inset Fig. 1a). Bacterial cells (10^5 CFU/mL) in PBS showed no absorption peak at 260 nm (Fig. 1a). When cells were incubated with Apt1 and then thoroughly washed, a significant increase in the intensity of the peak at 260 nm was observed indicating the binding of Apt1 to *S. aureus*. Control tests performed with bacterial cells incubated with a linear oligonucleotide sequence did not produce peak intensity increase at 260 nm (Fig. 1a).

3.2. Optimization of Apt1 working concentration. Citrate capped AuNPs (20 nm) used here were electrically stabilized and of a red color. By adding 5 µL of $MgCl_2$ of different concentrations to 50µL of AuNPs, the color change of the solution was observed by naked eyes when final concentrations of $MgCl_2$ were higher than 200 mM. In several minutes, at such high ionic strengths, the solution changed from red (plasmonic band was at ~520 nm) to a blue-to-violet color (plasmonic band was at ~ 630 nm) due to nanoparticle aggregation

191 (Fig. 1b). The aptamer adsorption on AuNPs may protect nanoparticles from salt-induced
192 aggregation (Marin et al. 2021). The working concentration of Apt1 was optimized to control
193 the stability of AuNPs by increasing the Apt1/AuNPs molar ratio (Fig. 1c). AuNPs rested
194 stabilized at a molar ratio above 150:1 after addition of $MgCl_2$. At these high ratios, Apt1
195 molecules adsorbed on AuNPs and prevented aggregation. The protection was weak for
196 lower the Apt1/AuNPs ratios and solutions of AuNPs changed to a violet color upon salt
197 addition (Fig. 1c). Therefore, the ratio 150:1 (0.1 µM Apt1 final concentration) and 200 mM
198 $MgCl_2$ were chosen for the aptasensor construction. The reaction time of 15 min was
199 sufficient to observe the color change, and was further used in experiments.

200 **3.3. Development of the assay for *S. aureus* detection.** Most reported aptasensors
201 based on AuNPs work in a direct target-mediated AuNPs aggregation mode (Marin et al.
202 2021). However, when we applied it to detection of *S. aureus*, this approach led to a
203 detection failure because nanoparticles adsorbed and aggregated on bacterial cells
204 regardless their functionalization, as shown in Fig. 2. Despite the fact that both AuNPs and
205 bacterial cells are of a negative surface charge, AuNPs seemed to bind bacterial cells by a
206 nonspecific adsorption and aggregate. This phenomenon was not influenced by the absence
207 and presence of Apt1 (Fig. 2). Moreover, the aggregation of non-functionalized AuNPs was
208 observed with another milk contaminating bacterium *B. cereus* (Fig. S-1), suggesting that
209 AuNPs may adsorb on other Gram-positive bacteria.

210 To eliminate the nonspecific binding between bacterial cells and AuNPs, an indirect assay
211 was performed as illustrated in Schema 1. In the first step Apt1 was added to the sample and
212 incubated for 10 min. In the absence of *S. aureus*, Apt1 diffused freely in the sample and
213 could not be removed by centrifugation. In the second step, supernatants were added to
214 AuNPs solution and aptamers prevented salt-induced aggregation. In contaminated samples

Apt1 precipitated with bacterial cells enabling AuNPs to aggregate upon salt addition. The color change thus occurred only for positive samples and could be observed visually or measured by a spectrophotometer and expressed by the A_{630}/A_{520} ratio.

We evaluated the performance of the colorimetric two-step aptasensor for the detection of *S. aureus* in pure culture. Prior to detection bacterial cells, cultivated in BHI medium, were washed and resuspended in PBS. Fig. 3 shows that as the concentration of bacterial cells increased, the absorbance ratio (A_{630}/A_{520}) gradually increased. The proposed two-step detection mode was highly sensitive: a visible color change of AuNPs from red to blue due to aggregation can be seen in inset Fig. 3. The limit of detection was 10^3 CFU/mL visually, and 1 CFU/mL by UV–vis Spectrum (obtained by the equation 3S/N, where S is the standard deviation of the blank solution, and N is the slope of the calibration curve, inset in Fig. 3). In addition, the dynamic range with a good linear response was obtained for *S. aureus* concentrations between 10^2 CFU/mL and 10^8 CFU/mL.

However, when this two-step assay was performed in inoculated milk and infant formula, the reactive solution color change was observed only for *S. aureus* at concentrations ≥ 10^8 CFU/mL. Milk components strongly interfered with the apta-sensor. Probably, bacterial cells absorbed many milk components that desorbed during the test and prevent AuNPs aggregation. To adapt the test to complex milk-based products and increase the test sensitivity we next sought to eliminate the inhibitory matrix effect.

3.4. Milk and infant formula treatment. In the aim to make the test as simple and cheap as possible, we compared different treatments that eliminate proteins in milk and allow AuNPs aggregation upon salt addition. The UV-Vis spectroscopy of milk and infant formula showed that both food matrices strongly adsorb in the visible wavelength region confirming that direct spectroscopic observation of AuNPs aggregation would not be possible (Fig. 4a).

Since Apt1 recognizes live bacterial cells the ideal treatment should eliminate the matrix effect without damaging bacterial cells. More than 80% of total milk proteins are caseins that together with a high proportion of calcium and phosphates are incorporated into lipidic micelles (Marathe et al. 2012). These proteins were denatured by addition of 2 % TCA, HCl to reach pH 3, or by using chelating agent EDTA alone or in combination with Triton-X100 to solubilize micelles (Fig. 4a and Fig. S-2). All tests were performed in samples containing *Bacillus cereus* cells. *B. cereus* of a characteristic rod-shape and size of a few microns was chosen for easy optical microscope observation. The TCA treatment was not adapted for direct LSPR assays because of TCA precipitated proteins that were pelleted together with bacterial cells. The HCl treatment efficiently denatured proteins and made the solution transparent but damaged bacterial cells. Finally, EDTA caused protein unfolding and denaturing by sequestering calcium ions and disturbing micelles without injuring bacterial cells. By adding a double volume of 15mM EDTA solution, solutions became transparent due to the milk protein unfolding (Makhzami et al. 2008), as illustrated in Fig. 4a. Interestingly, despite the fact that the infant formula sample was still of a white color (Fig. S-2) both EDTA-treated milk and infant formula showed no absorption in the visible region as presented in Fig. 4a. Similar efficiency to make the sample transparent was observed with the EDTA/Triton-X100 treatment (Fig. 4a). Triton-X100 was added to disperse fat flocculants containing proteins. For test simplicity, the EDTA treatment was chosen in further detection assays. Fig. 4b shows that EDTA addition to milk and infant formula containing AuNPs enabled naked-eye visualization of AuNPs aggregation upon salt addition. In contrast, no nanoparticle aggregation was observed in untreated samples.

To verify the non-toxicity of the EDTA treatment, analysis of the cytotoxic effects of the 15 mM EDTA on *S. aureus* was performed by enumeration of survival bacterial cells, and

using the LIVE/DEAD BacLight Kit in combination with epifluorescence microscopy. No decrease in the bacterial cell number was obtained in EDTA-treated milk and infant formula inoculated with 10^5 CFU/mL *S. aureus* compared to the corresponding untreated samples. After staining of *S. aureus* cells with a SYBR Green I and PI mixture, living bacterial cells were of green fluorescence, and dead cells of red fluorescence. Fig. 4c clearly shows that most round-shaped *S. aureus* cells were alive in samples containing EDTA. The non-toxicity of 15 mM EDTA was confirmed using *B. cereus* cells in milk and infant formula samples (Fig. S-3).

3.5. Analytical performance of the apta-sensor in complex matrices. Utilizing the optimized conditions, the LSPR apta-sensor shows a linear response to *S. aureus* over a dynamic range of 10^4-10^8 CFU/mL cells in milk and infant formula (Fig. 5). The theoretical limit of detection was $7.5x10^4$ CFU/mL and $8.4x10^4$ CFU/mL of *S. aureus* in milk and infant formula, respectively. The visual limit of detection was 10^6 CFU/mL of *S. aureus* (insets Fig. 5). Despite the fact that such detection performances are inferior to some recently reported for other aptamer-based biosensors (Abbaspour et al. 2015; Tao et al. 2021), this colorimetric biosensor has advantages to be instrument free and performed in complex food matrices. Moreover, in contrast to colorimetric sensors coupled to signal amplification, our two-step assay is not connected to instrumentations which often require complex biochip-processing technology or expensive filters and set-ups.

The selectivity of the colorimetric apta-sensor for *S. aureus* was tested by comparing the obtained color change with that of other interfering bacteria under the same conditions. The results in Fig. 6 show that only solution of milk and infant formula spiked with *S. aureus* had a violet color, and their absorption variation (A_{630}/A_{520}) was significantly higher than that obtained with non-relating bacteria. This finding strongly suggests that Apt1 did not bind to

control strains and, thus, Apt1 in supernatants could adsorb to AuNPs and prevented their aggregation.

4. CONCLUSION

In summary, we developed a milk and infant formula treatment to increase the sensitivity of a direct colorimetric detection of *S. aureus* using an apta-sensor based on LSPR and AuNPs. In the assay, contaminated samples were evidenced through AuNPs aggregation and solution color change that could be compromised by matrix proteins. Specifically, our study suggested that milk proteins even in traces may adsorb on gold nanoparticles and significantly decrease the assay sensitivity. The addition of EDTA solubilized milk and infant formula macromolecules, which boosted the sensitivity of *S. aureus* detection. The obtained limit of detection suggests that the apta-sensor is suitable for screening dairy samples for *S. aureus* since its ingested infectious doses were reported to be over 10^{10} cells (Jankie et al. 2016).

The EDTA treatment made the assay a promising alternative for the design of novel biosensors. In case of detection of other milk contaminating bacterial pathogens, such as *Campylobacter* or *Escherichia coli*, that have very low infectious doses (500 cells and 100 cells, respectively), the sensibility of the assay can be further improve by coupling AuNPs to an enzymatic reaction (Marin et al. 2021; Yuan et al. 2014) or other nanoparticles.

Abbreviations Used:

AuNPs, gold nanoparticles; BHI, brain-heart-infusion; EDTA, ethylenediaminetetraacetic acid; ELISA, enzyme-linked immunosorbent assay; LSPR, localized surface plasmon resonance;

MALDI-TOF, Matrix Assisted Laser Desorption Ionization - Time of Flight; PCR, polymerase chain reaction; PBS, phosphate buffered saline; TCA, trichloroacetic acid.

ASSOCIATED CONTENT

Supporting information

Binding of AuNPs to *B. cereus* cells (Figure S-1), photographs of milk and infant formula samples treated to denature milk macromolecules (Figure S-2), images of *B. cereus* cells collected from milk and infant formula solution after different treatments (Figure S-3) and LIVE/DEAD BacLight stain of *B. cereus* cells in EDTA-treated milk and infant formula solutions (Figure S-4).

Funding

This work is in a part supported by the French agency for research (ANR) for funding (Siena, ANR-21-CE21-0009-03), the DIM OneHealth2021 and the European Union's Horizon 2020 research and innovation programme under the Marie Skłodowska–Curie grant agreement N° 872662 (IPANEMA).

Acknowledgments

We acknowledge the MIMA2 platform for access to electron microscopy equipment (MIMA2, INRAE, 2018. Microscopy and Imaging Facility for Microbes, Animals and Foods, https://doi.org/10.15454/1.5572348210007727E12), Thierry Meylheuc (INRAE, France) for his expertise with scanning electron microscopy, Mayura Subramaniam (Université Paris-Sacaly, France) for technical assistance and Maria Vesna Nikolic (University of Belgrade, Serbia) for discussion and critical reading of the manuscript.

Author contribution:

M.M. helped to design research, performed part of the milk treatment research, and helped to write the article; F.R. performed the research, analyzed the data, and helped to write the article. V.L.

performed the research; C.P. performed transmission electron microscopy analyses, E.BD. help to design the research and edit article, and J.V. designed the research, performed experiments, analyzed the data, and wrote the article. All authors approved the final version of the article.

Notes

The authors declare no competing financial interest.

FIGURE LEGENDS:

Figure 1. (a) Spectrophotometric detection of Apt1 binding to *S. aureus* cells. The insert shows the adsorption spectra of Apt1. (b) Optimization of the molar ratio of Apt1 to AuNPs, mean ± SD of 3 measurements. The insert shows color changes of AuNPs solution at each ratio. (c) UV-Vis adsorption spectra of AuNPs before (stabilized AuNPs) and after $MgCl_2$ addition (aggregated AuNPs).

Figure 2. Transmission electron micrographs of *S. aureus* cells and (a) unmodified AuNPs and (b) AuNPs carrying adsorbed Apt1. Note that in both cases bacterial cells/nanoparticle aggregates were formed.

Schema 1. Graphical illustration of the designed two-stage detection of *S. aureus* using a colorimetric apta-sensor.

Figure 3. Photographed image and colorimetric detection of *S. aureus* in PBS. The calibration curve of adsorption ratio 630/520 nm versus concentration of *S. aureus*. Insert graph show the derived calibration curve for corresponding means ± SD of 3 experiments. Insert photograph shows color changes of AuNPs at each concentration.

Figure 4. (a) UV-Vis spectra of powder milk and infant formula water solutions before (Control1), and after inoculation with 10^5 CFU/mL *B. cerus* bacterial cells (Control2), and UV-Vis spectra of corresponding bacterial solutions treated with 15 mM EDTA (pH 8), 15 mM

EDTA/ 1% Triton X-100, HCl (pH 3) and 2% TCA. (b) Effect of EDTA treatment to visualization of the salt addition to AuNPs admixed to noncontaminated milk and infant formula solutions. (c) LIVE/DEAD BacLight stain of *S. aureus* cells in milk and infant formula treated with 15 mM EDTA, pH 8. Scale bar, 5 µm stains for all images.

Figure 5. Adsorption ratio at 630 and 520 nm of AuNPs versus concentration of *S. aureus* in inoculated milk and infant formula solutions. Insert graphs show the derived calibration curves for corresponding, means ± SD of 3 experiments. Insert photograph shows color changes of AuNPs at each concentration, where far-left and far-right wells correspond to negative control (2 µM Apt1) and positive control (no Apt1), respectively.

Figure 6. Visual color and the adsorption ratio at 630 and 520 nm of the sensing solutions for *S. aureus* (10^6 CFU/mL) and six interfering bacteria (10^7 CFU/mL), mean ± SD of 3 experiments.

References:

Abbaspour, A., Norouz-Sarvestani, F., Noori, A., Soltani, N., 2015. Aptamer-conjugated silver nanoparticles for electrochemical dual-aptamer-based sandwich detection of *Staphylococcus aureus*. Biosensors and Bioelectronics 68, 149-155.

Aura, A.M., D'Agata, R., Spoto, G., 2017. Ultrasensitive Detection of *Staphylococcus aureus* and *Listeria monocytogenes* Genomic DNA by Nanoparticle-Enhanced Surface Plasmon Resonance Imaging. Chemistryselect 2(24), 7024-7030.

Balbinot, S., Srivastav, A.M., Vidic, J., Abdulhalim, I., Manzano, M., 2021. Plasmonic biosensors for food control. Trends in Food Science & Technology. 111, 128-140

Bobrinetskiy, I., Radovic, M., Rizzotto, F., Vizzini, P., Jaric, S., Pavlovic, Z., Radonic, V., Nikolic, M.V., Vidic, J., 2021. Advances in Nanomaterials-Based Electrochemical Biosensors for Foodborne Pathogen Detection. Nanomaterials 11(10), 2700.

Chen, H., Zhou, K., Zhao, G., 2018. Gold nanoparticles: From synthesis, properties to their potential application as colorimetric sensors in food safety screening. Trends in Food Science & Technology 78, 83-94.

Cho, T.J., Hwang, J.Y., Kim, H.W., Kim, Y.K., Kwon, J.I., Kim, Y.J., Lee, K.W., Kim, S.A., Rhee, M.S., 2019. Underestimated risks of infantile infectious disease from the caregiver's typical handling practices of infant formula. Scientific reports 9(1), 1-12.

Cossettini, A., Vidic, J., Maifreni, M., Marino, M., Pinamonti, D., Manzano, M., 2022. Rapid detection of *Listeria monocytogenes*, *Salmonella*, *Campylobacter* spp., and *Escherichia coli* in food using biosensors. Food Control, 108962.

Duarte, C.M., Carneiro, C., Cardoso, S., Freitas, P.P., Bexiga, R., 2017. Semi-quantitative method for Staphylococci magnetic detection in raw milk. The Journal of dairy research 84(1), 80.

Eissa, S., Zourob, M., 2020. Ultrasensitive peptide-based multiplexed electrochemical biosensor for the simultaneous detection of *Listeria monocytogenes* and *Staphylococcus aureus*. Microchimica Acta 187(9), 1-11.

Hennekinne, J.-A., De Buyser, M.-L., Dragacci, S., 2012. Staphylococcus aureus and its food poisoning toxins: characterization and outbreak investigation. FEMS microbiology reviews 36(4), 815-836.

Holmes, M.A., Zadoks, R.N., 2011. Methicillin resistant *S. aureus* in human and bovine mastitis. Journal of mammary gland biology and neoplasia 16(4), 373-382.

Jankie, S., Jenelle, J., Suepaul, R., Pereira, L.P., Akpaka, P., Adebayo, A.S., Pillai, G., 2016. Determination of the infective dose of *Staphylococcus aureus* (ATCC 29213) and *Pseudomonas aeruginosa* (ATCC 27853) when injected intraperitoneally in Sprague Dawley rats. Journal of Pharmaceutical Research International, 1-11.

Kadariya, J., Smith, T.C., Thapaliya, D., 2014. *Staphylococcus aureus* and staphylococcal food-borne disease: an ongoing challenge in public health. BioMed research international 2014.

Kotsiri, Z., Vidic, J., Vantarakis, A., 2022. Applications of biosensors for bacteria and virus detection in food and water–A systematic review. Journal of Environmental Sciences 111, 367-379.

Kumar, N., Seth, R., Kumar, H., 2014. Colorimetric detection of melamine in milk by citrate-stabilized gold nanoparticles. Analytical biochemistry 456, 43-49.

Land, K.J., Boeras, D.I., Chen, X.-S., Ramsay, A.R., Peeling, R.W., 2019. REASSURED diagnostics to inform disease control strategies, strengthen health systems and improve patient outcomes. Nature microbiology 4(1), 46-54.

Lian, Y., He, F., Wang, H., Tong, F., 2015. A new aptamer/graphene interdigitated gold electrode piezoelectric sensor for rapid and specific detection of *Staphylococcus aureus*. Biosensors and Bioelectronics 65, 314-319.

Lund, T., De Buyser, M.L., Granum, P.E., 2000. A new cytotoxin from *Bacillus cereus* that may cause necrotic enteritis. Molecular microbiology 38(2), 254-261.

Makhzami, S., Quénée, P., Akary, E., Bach, C., Aigle, M., Delacroix-Buchet, A., Ogier, J.-C., Serror, P., 2008. In situ gene expression in cheese matrices: application to a set of enterococcal genes. Journal of Microbiological Methods 75(3), 485-490.

Marathe, S.A., Chowdhury, R., Bhattacharya, R., Nagarajan, A.G., Chakravortty, D., 2012. Direct detection of *Salmonella* without pre-enrichment in milk, ice-cream and fruit juice by PCR against hilA gene. Food Control 23(2), 559-563.

Marin, M., Nikolic, M.V., Vidic, J., 2021. Rapid point-of-need detection of bacteria and their toxins in food using gold nanoparticles. Comprehensive Reviews in Food Science and Food Safety n/a(n/a).

Martins, S.A., Martins, V.C., Cardoso, F.A., Germano, J., Rodrigues, M., Duarte, C., Bexiga, R., Cardoso, S., Freitas, P.P., 2019. Biosensors for on-farm diagnosis of mastitis. Frontiers in bioengineering and biotechnology 7, 186.

Nouri, A., Ahari, H., Shahbazzadeh, D., 2018. Designing a direct ELISA kit for the detection of *Staphylococcus aureus* enterotoxin A in raw milk samples. International journal of biological macromolecules 107, 1732-1737.

Quigley, L., O'Sullivan, O., Stanton, C., Beresford, T.P., Ross, R.P., Fitzgerald, G.F., Cotter, P.D., 2013. The complex microbiota of raw milk. FEMS microbiology reviews 37(5), 664-698.

Rajkovic, A., Jovanovic, J., Monteiro, S., Decleer, M., Andjelkovic, M., Foubert, A., Beloglazova, N., Tsilla, V., Sas, B., Madder, A., 2020. Detection of toxins involved in foodborne diseases caused by Gram-positive bacteria. Comprehensive Reviews in Food Science and Food Safety 19(4), 1605-1657.

Ramarao, N., Tran, S.-L., Marin, M., Vidic, J., 2020. Advanced methods for detection of *Bacillus cereus* and its pathogenic factors. Sensors 20(9), 2667.

Rubab, M., Shahbaz, H.M., Olaimat, A.N., Oh, D.-H., 2018. Biosensors for rapid and sensitive detection of *Staphylococcus aureus* in food. Biosensors and Bioelectronics 105, 49-57.

Rüppel, N., Tröger, V., Sandetskaya, N., Kuhlmeier, D., Schmieder, S., Sonntag, F., 2018. Detection and identification of *Staphylococcus aureus* using magnetic particle enhanced surface plasmon spectroscopy. Engineering in Life Sciences 18(4), 263-268.

Ryu, S., Song, P.I., Seo, C.H., Cheong, H., Park, Y., 2014. Colonization and infection of the skin by *S. aureus*: immune system evasion and the response to cationic antimicrobial peptides. International journal of molecular sciences 15(5), 8753-8772.

Schlag, S., Nerz, C., Birkenstock, T.A., Altenberend, F., Götz, F., 2007. Inhibition of staphylococcal biofilm formation by nitrite. Journal of bacteriology 189(21), 7911-7919.

Schrader, C., Schielke, A., Ellerbroek, L., Johne, R., 2012. PCR inhibitors–occurrence, properties and removal. Journal of applied microbiology 113(5), 1014-1026.

Tao, X., Chang, X., Wan, X., Guo, Y., Zhang, Y., Liao, Z., Song, Y., Song, E., 2020. Impact of protein corona on noncovalent molecule–gold nanoparticle-based sensing. Analytical Chemistry 92(22), 14990-14998.

Tao, X., Liao, Z., Zhang, Y., Fu, F., Hao, M., Song, Y., Song, E., 2021. Aptamer-quantum dots and teicoplanin-gold nanoparticles constructed FRET sensor for sensitive detection of *Staphylococcus aureus*. Chinese Chemical Letters 32(2), 791-795.

Vidic, J., Chaix, C., Manzano, M., Heyndrickx, M., 2020. Food Sensing: Detection of *Bacillus cereus* Spores in Dairy Products. Biosensors 10(3), 15.

Vidic, J., Manzano, M., 2021. Electrochemical biosensors for rapid pathogen detection. Current Opinion in Electrochemistry, 100750.

Vidic, J., Manzano, M., Chang, C.-M., Jaffrezic-Renault, N., 2017. Advanced biosensors for detection of pathogens related to livestock and poultry. Veterinary research 48(1), 1-22.

Vidic, J., Vizzini, P., Manzano, M., Kavanaugh, D., Ramarao, N., Zivkovic, M., Radonic, V., Knezevic, N., Giouroudi, I., Gadjanski, I., 2019. Point-of-need DNA testing for detection of foodborne pathogenic bacteria. Sensors 19(5), 1100.

Vizzini, P., Braidot, M., Vidic, J., Manzano, M., 2019. Electrochemical and optical biosensors for the detection of *Campylobacter* and *Listeria*: An update look. Micromachines 10(8), 500.

Xu, L., Liang, W., Wen, Y., Wang, L., Yang, X., Ren, S., Jia, N., Zuo, X., Liu, G., 2018. An ultrasensitive electrochemical biosensor for the detection of mecA gene in methicillin-resistant *Staphylococcus aureus*. Biosensors and Bioelectronics 99, 424-430.

Yuan, J., Wu, S., Duan, N., Ma, X., Xia, Y., Chen, J., Ding, Z., Wang, Z., 2014. A sensitive gold nanoparticle-based colorimetric aptasensor for *Staphylococcus aureus*. Talanta 127, 163-168.

Zhang, F., Liu, J., 2021. Label-Free Colorimetric Biosensors Based on Aptamers and Gold Nanoparticles: A Critical Review. Analysis & Sensing 1(1), 30-43.

Graphic for Table of contents

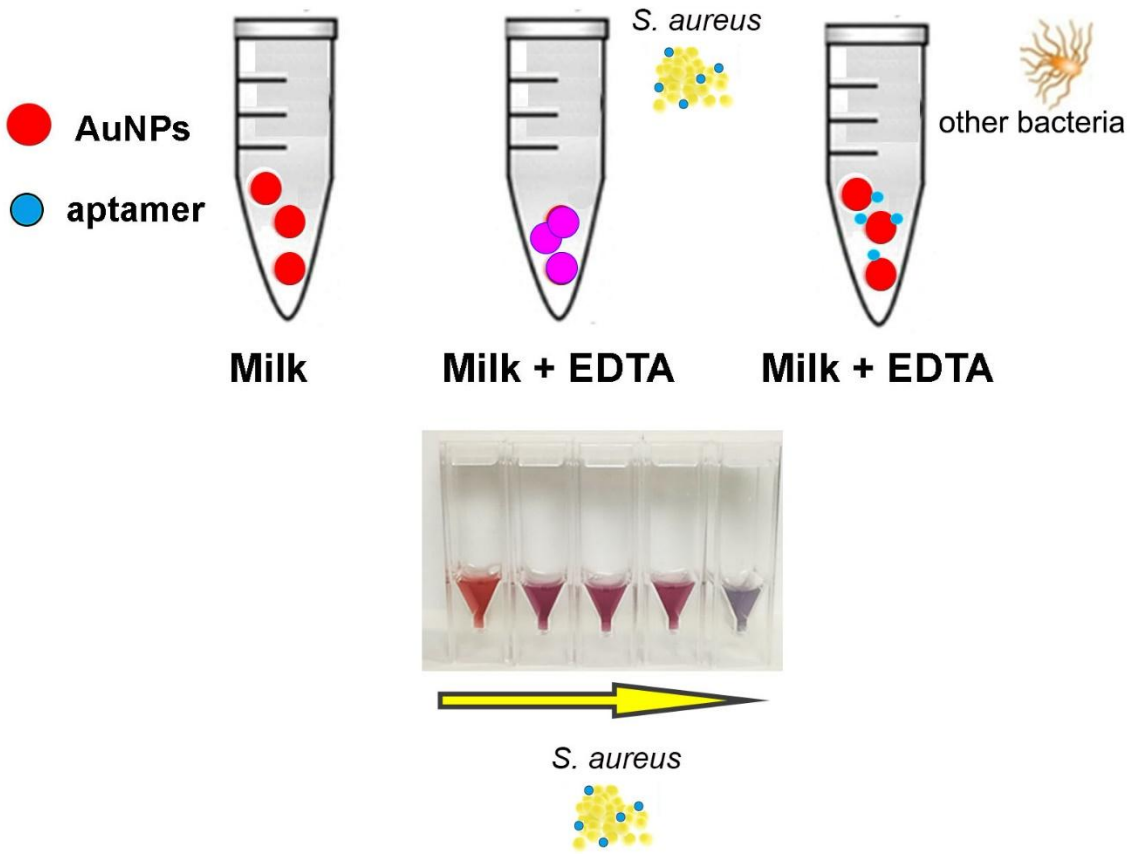

518

519